

On the Preparations of Magnetic Metal-Oxides (I)

(Solubilities of Sand-iron and Spongy-iron in Acids, and their Oxidation by Air-Blow)

SAKUJIRO YAMAMOTO

Summary

For the preparations of ferric oxide and ferrous-ferric oxide as the primary materials for ferrite magnets and magnetic metal-oxide for tape recording, the fine sand-iron and the special spongy-iron produced at TORIGAMI BRANCH FACTORY and at the METALLURGICAL LABORATORY of HITACHI-INZOKU Co., YASUGI are used respectively. The distributions of the particle-sizes of sand-iron, the iron contents by each grade of their particle-sizes, the solubilities of sand-iron and spongy-iron in hydrochloric acid and sulphuric acid, and then the effects of temperature on them are fundamentally researched.

Experiment and Discussion

(I) Treatments of Sand-iron and spongy-iron with acids.

(1) Sand-iron and spongy-iron used.

Table 1 gives the distribution of particle-sizes of the sand-iron corrected from the River Hii. Fig. 1 and Fig. 2 indicate the iron contents of each particle and their chemical constituents respectively; it is unexpectedly found so small that about half of the sand-iron has the size range in 200 mesh, and iron contents are rather larger in smaller particles than in larger ones. Iron is measured volumetrically with standardized $N_2S_2O_8$ solution.¹⁾

Table 1. Fe in sand-iron by particle-size

particle-size	mch 240	mch 240-200	mch 180-160	mch 160-140	mch 140-120
Fe					
%	74.0	74.0	72.6	72.6	72.6

Table 2. Chemical analysis of samples.

component sample	T. Fe	FeO	Fe ₂ O ₃	M. Fe	P	S	SiO ₂	TiO ₂	Al ₂ O ₃	CaO
sand-iron	73.50	31.09	61.98	—	0.100	Tr.	1.40	3.45	0.26	1.31
spongy-iron ※	89.70	7.50	0.50	85.50	0.105	0.108	—	4.85	—	—

※ mean values of seven samples

The chemical analysis of spongy iron is done with samples passed through 100 mesh, of sieve, and its data are given in Table 2.

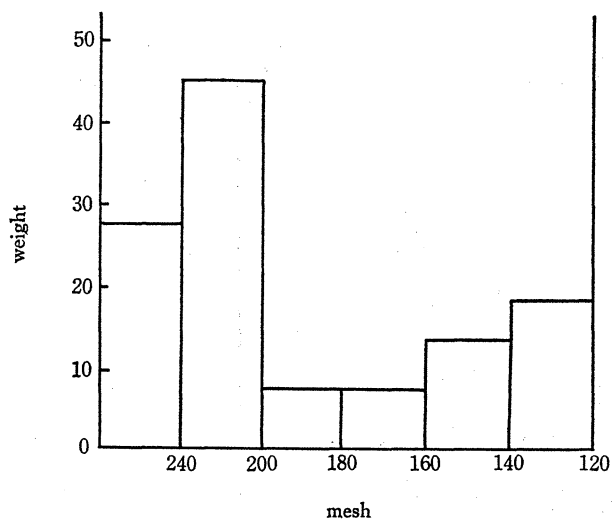


Fig. 1. Distribution of particles of sand-iron

(A) Hydrochloric acid

The Fig. 2—Fig. 5 give their characteristic solubilities of sand-iron and spongy-iron in 4N-and 12N-HCL. Sand-iron, when trieted in 12N-HCL at 100°C for 30 min. and in 4N-HCL at 100°C 30 min., has almost the same solubilities (80%). For spongy-iron, the effects of HCL concentration on the solubilities are remarkable ; in the diluted HCL solution, the solubilities of spongy-iron are smaller than those of sand-iron, but in the concentrated solution, they amount to 96.5% at 100°C for 90 min.,

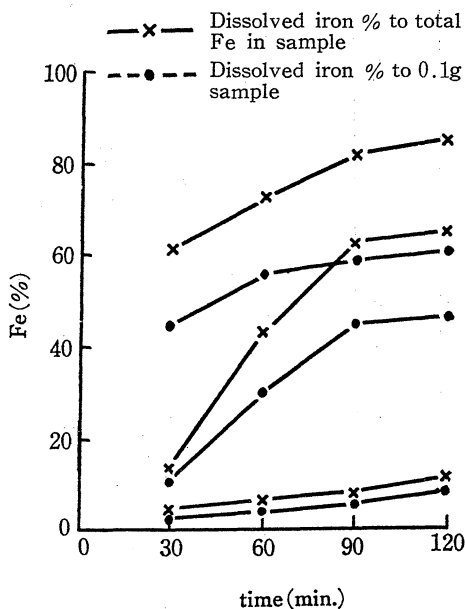


Fig. 2. Solubility of Fe in sandiron into 4 N-HCl sol.

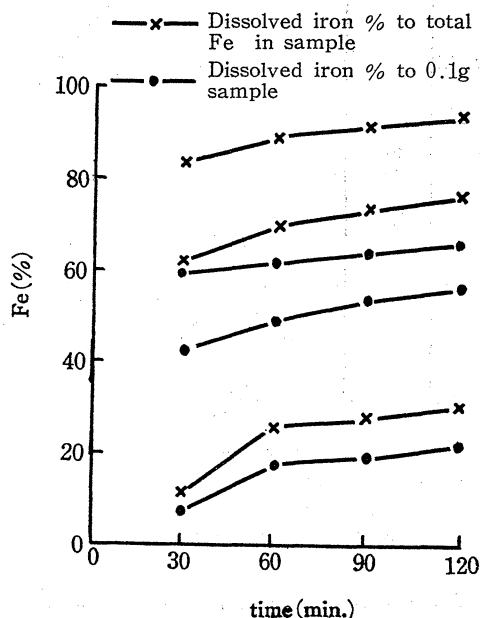


Fig. 3. Solubility of Fe in sandiron into 12 N-HCl sol.

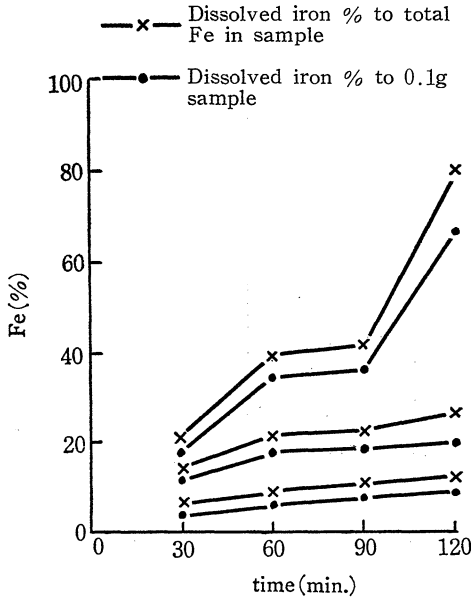


Fig. 4. Solubility of Fe in spongyiron into 4 N-HCl sol.

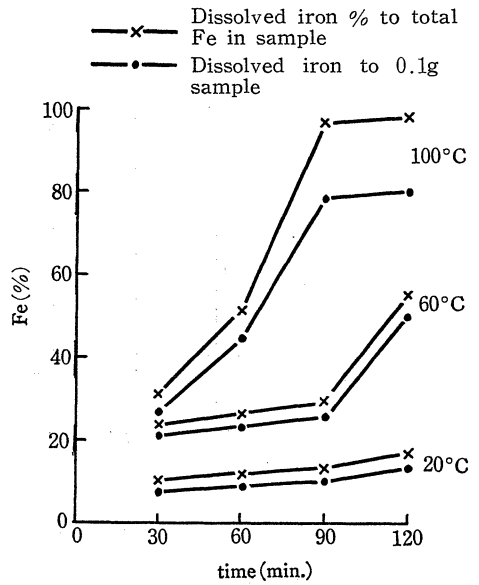


Fig. 5. Solubility of Fe in spongy-iron into 12 N-HCl sol.

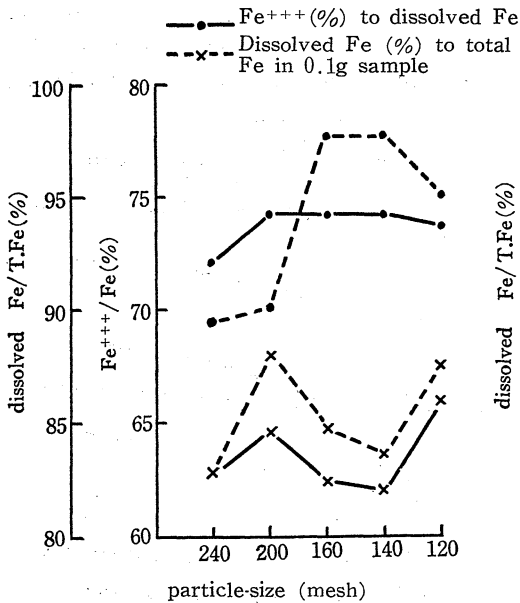


Fig. 6. Characteristic solubility of Fe in sand-iron into 12 N-HCl sol. by particle-size at 20°C.

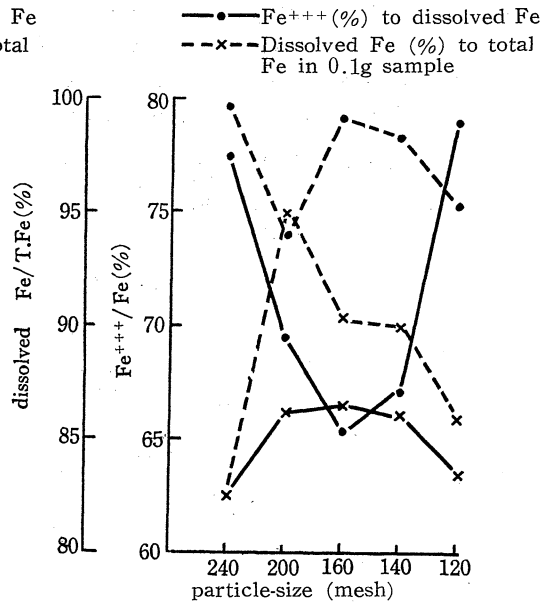


Fig. 7. Characteristic solubility of Fe in sand-iron into 12 N-HCl sol. by particle-size at 60°C.

The fig. 6 and Fig. 7 give the solubilities of sand-iron in HCL solution ; by their paticlesizes there are no appreciable effects of temperature and time on the solubilities of 200 mesh sample, but the 200 mesh sample allows the much increase of the dissolution

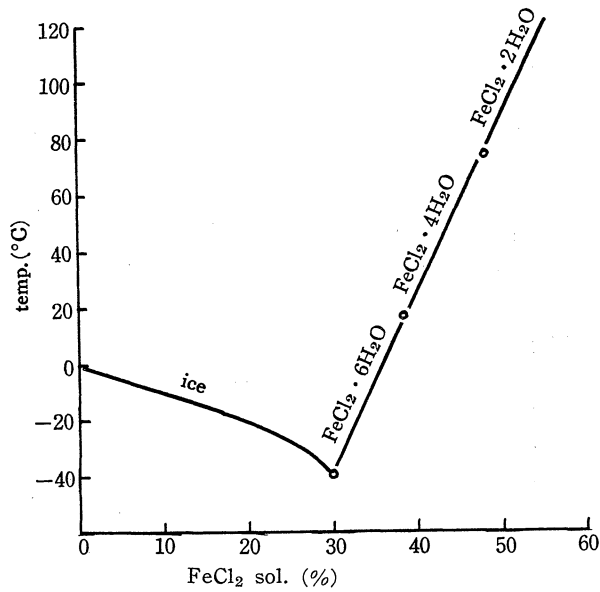


Fig. 8. Solubility curve of ferrous chloride.

of iron with the elevation of temperature and the elapse of time. It is not recognized that there is possible precise inclination of the increase of the concentration of Fe⁺⁺⁺ by the particle-sizes, but increase somewhat by the elapse of time ; it is considered that the oxygen dissolved in the solution oxidises Fe⁺⁺ to Fe⁺⁺⁺. The solubility of ferrous chloride in water increases with the elevation of temperature as in Fig. 8.²⁾

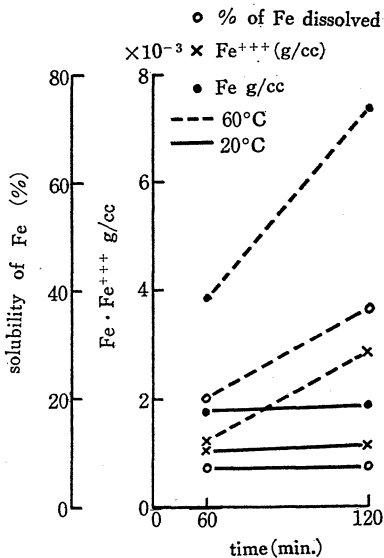


Fig. 9. Characteristic solubility of Fe in sand-iron into 12 N-H₂SO₄ sol. (Sample 0.02g/cc, 240~200 mesh)

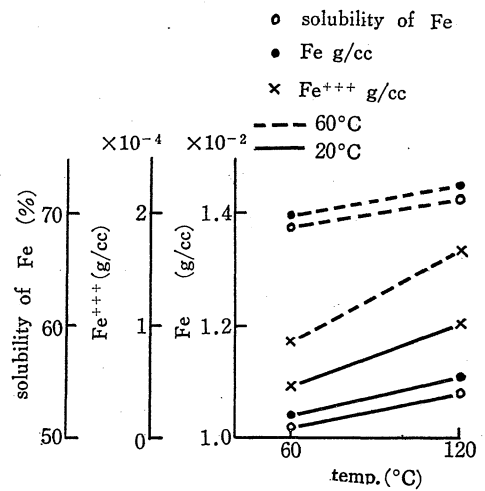


Fig. 10. Characteristic solubility of Fe in spongy-iron into 12 N-H₂SO₄ sol. (sample 0.2g/cc, 240~200 mesh)

(B) Sulphuric acid

The Fig. 9 and Fig. 10. give the characteristic solubility curves of sand-iron and spongy-iron in 4N-H₂SO₄ solution.

Sand-iron dissolves in H₂SO₄ less than half in HCL, and the concentration of Fe⁺⁺⁺ is very low or zero. Spongy-iron dissolves easier into H₂SO₄ than sand-iron, but reverse into HCL, giving no Fe⁺⁺⁺ in both solutions. It is already known that the characteristic solubility of ferrous sulphate in water is in the fact that the maximum solubility of it is in the vicinity of 60°C on the solubility-temperature curve given in Fig. 2.³⁾

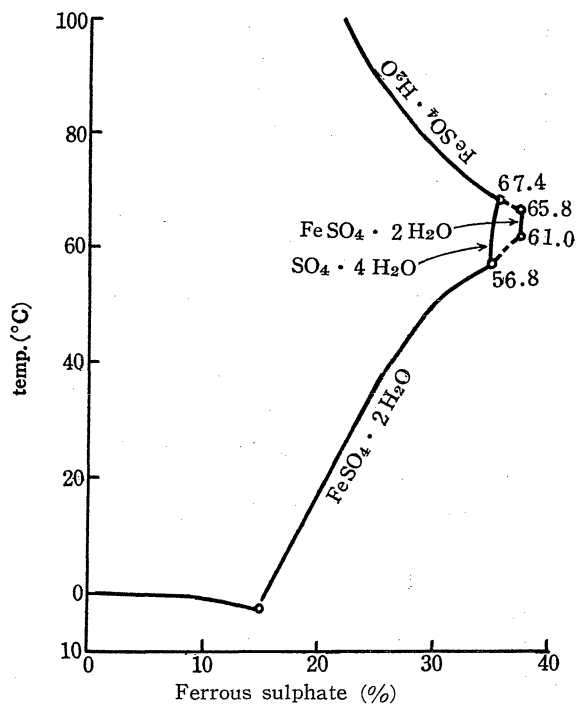


Fig. 11 Solubility curve of ferrous sulphate in water

(II) Air-oxidation of water solutions of iron salts.

(1) Ferrous Chloride

When each of the almost neutral solutions containing Fe⁺⁺⁺, obtained by dissolving sand-iron and spongy-iron in HCL respectively, which are controlled to be in the concentration of sample 0.1g/cc, is treated with air blow (1l/min.), the Fe⁺⁺ is oxidized slowly to Fe⁺⁺⁺; and the functional effect of the size of particles, temperature and time are indicated in Fig. 12—Fig. 14. In the case of sand-iron, the particles of 140–240 mesh are markedly soluble and oxidizable comparing with particles of the smaller and the larger mesh at 20°C for 60 min., and it is an interesting fact that for the 120–140 mesh particles, the Fe⁺⁺⁺/Fe values measured before and after air-blow at 20°C for 60 min., concentrate to the same point; and it is undoubtedly considered that in the case of 120–140 mesh particles; under these experimental conditions, the rates of the

disolution of sand-iron in HCL and of the oxydation of Fe^{++} to Fe^{+++} are parallel one another or the same. In the same series of experiments, if each particles of sand-iron is treated at $60^{\circ}C$, the dissolution and oxydation rates are extremely irregular with the exception of the fact that the concentration of those Fe^{+++}/Fe values in the 120–140 mesh particles is similar to the case of $20^{\circ}C$.

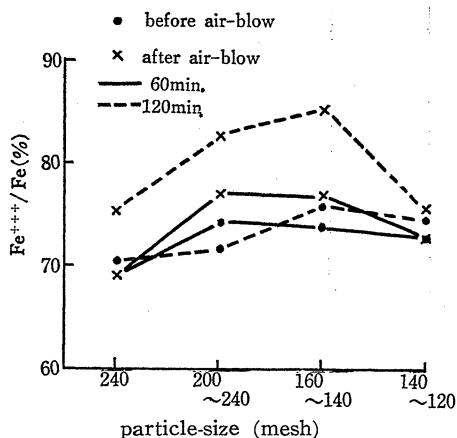


Fig. 12. Oxydation of HCl sol. of sand-iron by air-blow. ($20^{\circ}C$, 11 air/min., 0.1g/cc)

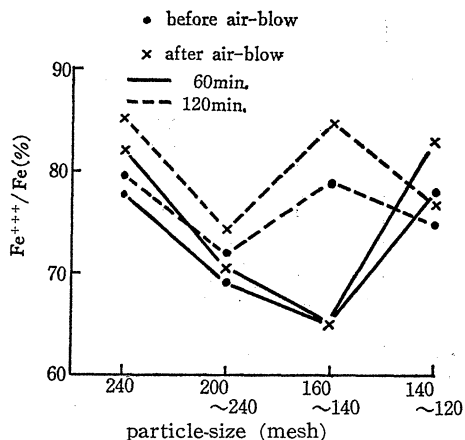


Fig. 13. Oxydation of HCl sol. of sand-iron by air-blow. ($60^{\circ}C$, 11 air/min.)

In the case of spongy-iron, the differences of particle-size and temperature affect regularly the rate of oxydation of Fe^{++} to Fe^{+++} ; the oxydation of rough particles proceeds rapidly, and that of fine ones very slowly.

The air-oxydation curve of the mixed solution of $FeCl_2$ and $FeCl_3$ in the hydrochloric acid solution is given in Fig. 15. Fig. 16.

The pure ($FeCl_2 + FeCl_3$) solution and the pure $FeCl_2$ solution correspond to those of sand-iron and spongy-iron respectively. In the latter case, with the increase of the concentration of HCL, in spite of the slight absolute increase of Fe^{+++} , the Fe^{+++}/Fe value somewhat elevate, but it falls in the former case.

From these results it can be known that the rate of oxydation of Fe^{++} to Fe^{+++} by air-blow is minus regulated with the higher concentration of the co-existing Fe^{+++} , and the higher the concentration of HCL elevate, the lower the Fe^{+++}/Fe value becomes. Accordingly, it will be expected that, for instance, it must need much more time to oxydize Fe^{++} to Fe^{+++} for the formation of $\alpha-FeO.OH$ or $\gamma-Fe.OH$ in the wet method.

The oxydation ionpower of air-blow is calculated as follows ;

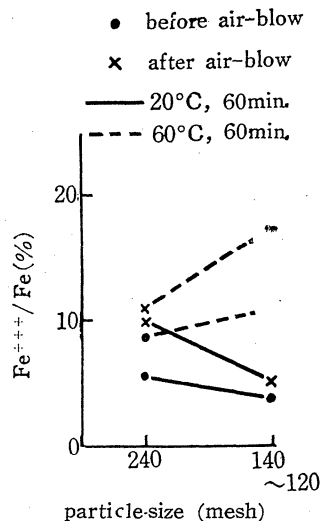


Fig. 14. Oxydation of HCl sol. of spongy iron by air-blow (0.1g/cc, 11 air/min.)

$$\frac{C_{\text{Fe}^{+++}}(\text{after air-blow}) - C_{\text{Fe}}(\text{before air-blow})}{\text{total Fe}} \times 100(\%)$$

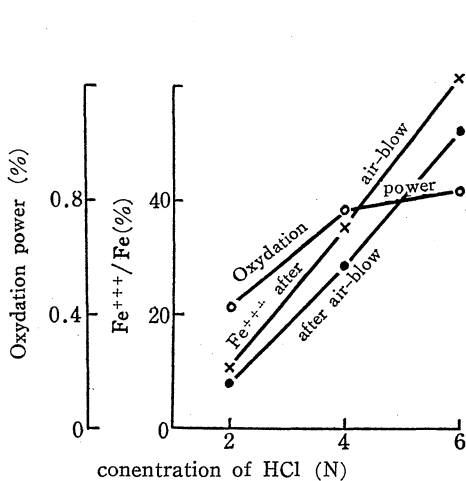


Fig. 15. Oxidation of HCl- FeCl_2 sol. at 20°C (11 air/min., 2 mol. FeCl_2 sol. total volume 80cc.)

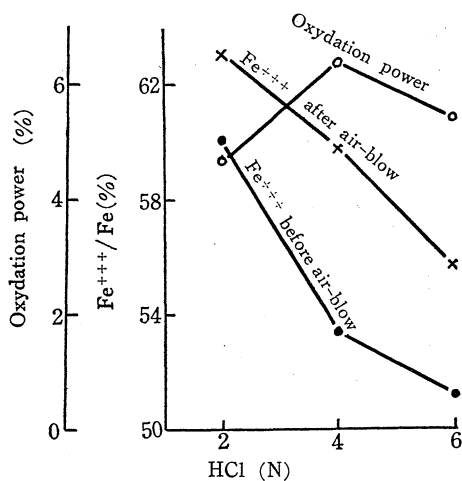


Fig. 16. Oxidation of $(\text{FeCl}_2 + \text{FeCl}_3)$ sol. by air-blow. (11 air/min., 2 mol $\text{FeCl}_2 + 2$ mol FeCl_3 , total volume 80cc.)

(2) Ferrous Sulphate

According to the above experiments, sand-iron and spongy-iron are treated with H_2SO_4 instead of HCl, as dissolving agents. (Fig. 17—Fig. 18) The particlesizes of samples are in 200–240 mesh. In the case of sand-iron, it is easily seen that the $\text{Fe}^{+++}/\text{Fe}$ values obtained before and after the air-oxidation at 20°C are very close, independent of temperature, but the intervals of air-blow give a great effect on them. (Fig. 17)

On the contrary, the elevation of temperature from 20°C to 60°C lets the $\text{Fe}^{+++}/\text{Fe}$ value increase remarkably (about 40%), indicating the oxidation rate of Fe^{++} to Fe^{+++} is to be rapidly promoted by air-blow and not the elaps of time.

In the case of spongy-iron, it offers quite different conditions as shown in Fig. 18, namely the great differences (40%–45%) are found between the values before and after air-blow, which are likely to be independent of the temperature and of the intervals of air-blow. (Fig. 18)

The air-blow effects in the solution of $\text{FeSO}_4 \cdot 7\text{H}_2\text{O}$ and the (1 mol. $\text{FeSO}_4 + 0.39$ mol. $\text{Fe}_2(\text{SO}_4)_3$) mixed solution are shown in Fig. 19 and Fig. 20.

As the ferrous solution contains no Fe^{+++} , the concentration of Fe^{+++} titrated after air-blow mean the oxidation power for itself. The higher acid concentration elevates, the higher oxidation power become.

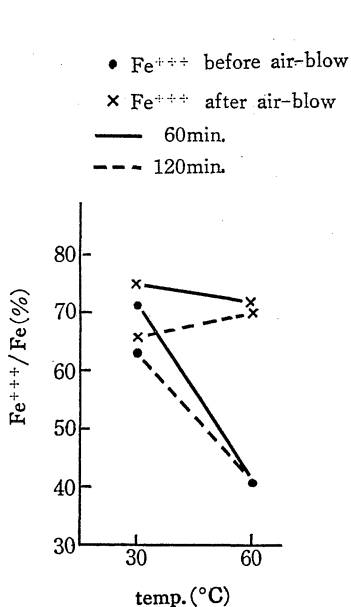


Fig. 17 Oxydation of Fe in H₂SO₄ acidic sol. of sand-iron by air-blow at 20°C. (11 air/min., 240~200mesh.)

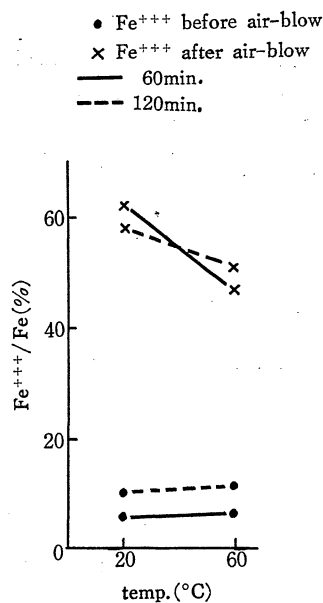


Fig. 18. Oxydation of Fe in H₂SO₄ acidic sol. of spongy-iron by air-blow at 20°C. (11 air/min., 240~200 mesh.)

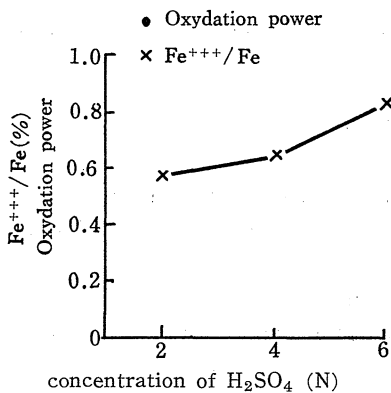


Fig. 19. Oxydation of FeSO₄ in H₂SO₄ acidic sol. by air-blow at 20°C. (1mol. FeSO₄·7H₂O sol., T. V. 60 cc, 11 air/min.)

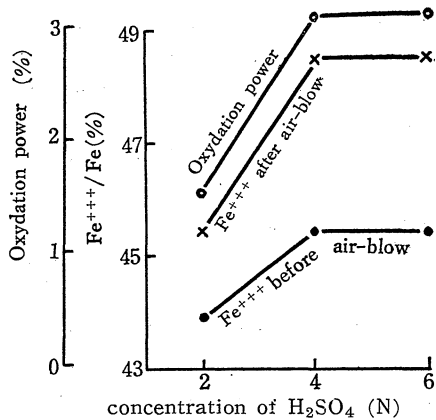


Fig. 20. Oxydation of Fe in H₂SO₄ acidic [FeSO₄+0.39 Fe₂(SO₄)₃] sol. by airblow. at 20°C. (2 mol. FeSO₄·7H₂O+1.8g Fe₂(SO₄)₃: Fe⁺⁺: e⁺⁺⁺=56.05:43.95=1 : 0.78, T. V. 60cc, 11 air/min.

References

- 1) S. YAMAMOTO. "NIHONKAGAKUKAI-ZASSHI" 73, 22-31 (1952).
S. YAMAMOTO. *ibid.*, 74 9-13 (1953).
- 2) T. INOUE. ; "RIKAGAKU-ZITEN", IWANAMI, (1953).
- 3) M. MORI, ; "KŌTŌ-KAGAKU-SHINRO N", vol., III, USHIDA-RŌKAKUHO (1944).